

## ESI Electronic Supplementary Information

### ESI.1 Choosing a functional

To choose an appropriate functional for the exchange and correlation energy, we determined the equilibrium lattice parameter  $a_0$  and the cohesive energy  $E_{\text{coh}}$  of gold for several common functionals. As compared to other exchange-correlation functionals, the PBE-D3 functional leads to the values for both quantities which agree very well with experiment (see Table ES1).

**Table ES1** Lattice constants  $a_0$  and cohesive energy  $E_{\text{coh}}$  for different exchange-correlation functionals in comparison to literature values.

Functional	$a_0$ [Å]	$E_{\text{coh}}$ [eV/atom]
LDA	4.052	4.31
PBE	4.156	3.04
vdWopt86b	4.121	3.76
PBE+D2	3.996	4.53
PBE+D3	4.099	3.70
experiment	4.072 <sup>1</sup>	3.81 <sup>2</sup>

### ESI.2 Reconstruction of the clean Au(321) surface under oxidation

When the infinite oxide chain is formed, two atoms of the clean Au(321) surface undergo significant vertical displacements out of the surface to bond with the two O atoms and build the chain going across the steps. Surrounding Au atoms are also slightly displaced vertically and horizontally in the process. Fig. ES1 compares the clean and the oxidized surface and gives the largest values and directions of displacements. The clean reference structure is depicted with gray atoms, while the final surface configuration is shown in gold Au and red O atoms.

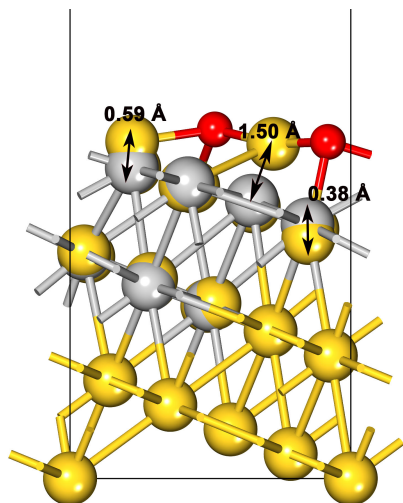


**Fig. ES1** Reconstruction of the clean Au(321) surface under formation of the infinite oxide chain. Initial Au positions are depicted in grey, final Au positions in gold and O atoms in red.

### ESI.3 Influence of the exchange-correlation functional on the thermodynamic stability of bimetallic surfaces

The choice of the exchange-correlation functional may change absolute values of formation enthalpies, but as long as the obtained hierarchy and therefore the energetic preference of one structure over the other remains the same, the qualitative result is valid. Table ES2 shows the surface formation enthalpies  $\Delta H_f^{\text{surf}}$  of different structures at the same Ag surface concentration  $x_{\text{Ag}}^{\text{surf}} = 35.7\%$ , which was chosen arbitrarily, for PBE and PBE with dispersion corrections (D3). Their numbers arise from the enumeration algorithm implemented in the UNCLE code. The energetically most favorable structure is the same for both functionals, while the overall hierarchy remains with some small deviations. We therefore conclude that adding the D3 dispersion corrections to the PBE results should not have any impact on the qualitative results from our study.

**Table ES2** Surface formation enthalpies  $\Delta H_f^{\text{surf}}$  of selected structures at  $x_{\text{Ag}}^{\text{surf}} = 35.7\%$  for PBE and PBE+D3.

Structure no.	$\Delta H_f^{\text{surf}}$ [meV]	
	PBE	PBE+D3
7848	-27.5	-20.0
16036	-25.9	-19.8
7908	-25.0	-19.7
8100	-21.8	-19.1
15528	-22.4	-18.6
7080	-21.8	-17.0
16260	-17.6	-16.2
11056	-16.7	-13.2
16	-6.1	-6.9

### ESI.4 Segregation profiles

The Ag concentration  $x_{\text{Ag}}^{\text{layer}}$  within the surface and subsurface layer is presented in Fig. ES2. The surface layer was defined in such a way that it includes only metal atoms that do not have another atom on top of them. In line with this definition, each layer consists of six atoms. In both the surface and the subsurface layers,  $x_{\text{Ag}}^{\text{layer}}$  increases approximately linearly with increasing Ag surface concentration. For  $x_{\text{Ag}}^{\text{surf}} < 0.5$ , the Ag concentration at the surface is higher than in the subsurface layer, consistent with the tendency for Ag segregation near the oxide chains. However, for  $x_{\text{Ag}}^{\text{surf}} > 0.5$ , the two curves cross and the Ag concentration in the subsurface layer becomes larger than that of the surface layer, because from this point on, no further direct Ag–O contacts can be created and also all low-coordinated surface atoms are already substituted by Ag. At the same time, substitution of Au within the oxide chain is clearly unfavorable and occurs only at high Ag concentrations.

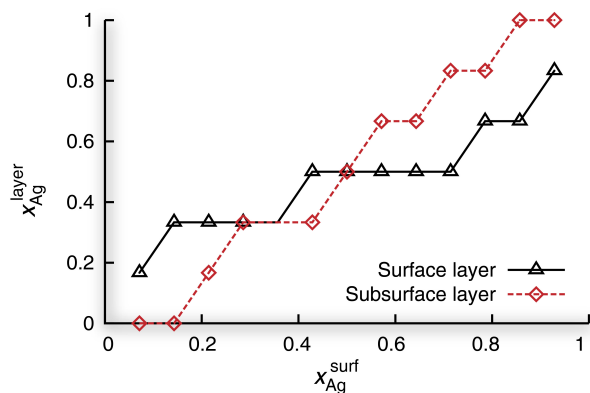


**Fig. ES2** Ag concentration in the surface and subsurface layer for ground states at all Ag surface concentrations.

### ESI.5 COHP analysis

A crystal orbital Hamilton population (COHP) analysis<sup>3,4</sup> partitions the band structure energy into bonding, nonbonding and antibonding contributions, where a negative value of the COHP corresponds to bonding energy regions and a positive value indicates antibonding interactions. The COHP analysis in this study was carried out with the program code Lobster<sup>5-7</sup>. In Fig. ES3, the negative average COHP between Ag and O atoms and Au and O atoms within the oxide chain, respectively, is plotted alongside the partial DOS. The filled area under the COHP curve on the right-hand side corresponds to bonding contributions, while the left-hand side represents antibonding contributions. The Fermi energy is indicated with a horizontal line. For both Ag and Au within the chain, we obtain two groups of filled bonding and partially filled antibonding states below the Fermi level. This picture is consistent with low lying completely filled *d*-bands of Au and Ag. As suggested by the partial DOS, these two groups are composed of the bonding and antibonding states between Au and O. The attractive interaction between O and Au/Ag arises from filling the bonding states and emptying some of the antibonding states. However, the peak resonances for the  $-(O-Au)-$  chain are much more pronounced than for the  $-(O-Ag)-$  chain, hinting towards a more covalent bonding character of the former. Furthermore, the bonding states for the  $-(O-Au)-$  chain lie at lower energy values than those of the  $-(O-Ag)-$  chain, leading to a larger gap between bonding and antibonding peaks, which is indicative of a stronger orbital interaction.

## References

- 1 I.-K. Suh, H. Ohta and Y. Waseda, *J. Mater. Sci.*, 1988, **23**, 757.
- 2 C. Kittel, *Introduction to Solid State Physics*, NJ: John Wiley & Sons, 8th edn., 2004.
- 3 R. Dronskowski and P. E. Blöchl, *J. Phys. Chem.*, 1993, **97**, 8617.

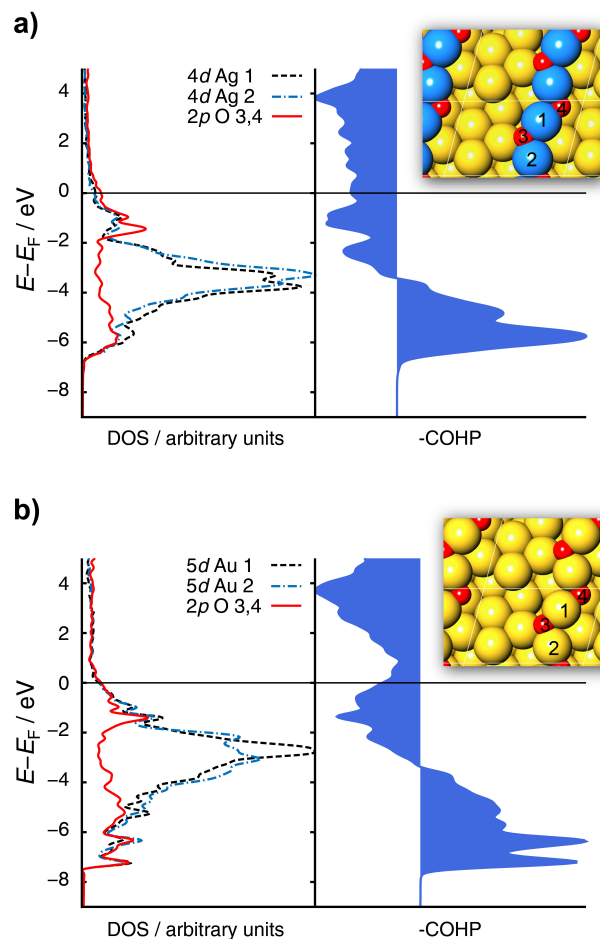


**Fig. ES3** Partial DOS and COHP analysis for the structure with  $-(O-Ag)-$  chain (a) and the structure with  $-(O-Au)-$  chain (b).

- 4 V. L. Deringer, A. L. Tchougreff and R. Dronskowski, *J. Phys. Chem. A*, 2011, **115**, 5461.
- 5 S. Maintz, V. L. Deringer, A. L. Tchougreff and R. Dronskowski, *J. Comput. Chem.*, 2013, **34**, 2557.
- 6 S. Maintz, V. L. Deringer, A. L. Tchougreff and R. Dronskowski, *J. Comput. Chem.*, 2016, **37**, 1030.
- 7 S. Maintz, M. Esser and R. Dronskowski, *Acta Phys. Pol. B*, 2016, **47**, 1165.